Quaternary Science Reviews 281 (2022) 107449

Contents lists available at ScienceDirect

Quaternary Science Reviews

journal homepage: www.elsevier.com/locate/quascirev

Anthropogenic warming reduces the carbon accumulation of Tibetan Plateau peatlands

Jianbao Liu [a, b, c, *, 1], Hanxiang Liu [a, b, 1], Huai Chen [d, b, 1], Zicheng Yu [f, g], Shilong Piao [b, e], John P. Smol [h], Jifeng Zhang [a, b], Lingxin Huang [c], Tao Wang [a, b], Bao Yang [i], Yan Zhao [j], Fahu Chen [a, b, c]

[a] State Key Laboratory of Tibetan Plateau Earth System Science (LATPES), Institute of Tibetan Plateau Research, Chinese Academy of Sciences, Beijing, 100101, China
[b] CAS Center for Excellence in Tibetan Plateau Earth Sciences, Chinese Academy of Sciences (CAS), Beijing, 100101, China
[c] Key Laboratory of Western China's Environmental Systems (Ministry of Education), College of Earth and Environmental Science, Center for Pan Third Pole Environment (Pan-TPE), Lanzhou University, Lanzhou, 730000, China
[d] Key Laboratory of Mountain Ecological Restoration and Bioresource Utilization & Ecological Restoration and Biodiversity Conservation Key Laboratory of Sichuan Province, Chengdu Institute of Biology, Chinese Academy of Sciences (CAS), Chengdu, 610041, China
[e] Sino-French Institute for Earth System Science, College of Urban and Environmental Sciences, Peking University, Beijing, 100871, China
[f] Key Laboratory of Geographical Processes and Ecological Security in Changbai Mountains (Ministry of Education), School of Geographical Sciences, Northeast Normal University, Changchun, 130024, China
[g] Department of Earth and Environment Sciences, Lehigh University, Bethlehem, PA, 18015, USA
[h] Paleoecological Environmental Assessment and Research Lab (PEARL), Department of Biology, Queen's University, Ontario, Kingston, K7L 3N6, Canada
[i] Key Laboratory of Desert and Desertification, Northwest Institute of Eco-Environment and Resources, Chinese Academy of Sciences (CAS), Lanzhou, 73000, China
[j] Key Laboratory of Land Surface Pattern and Simulation, Institute of Geographic Sciences and Natural Resources Research, Chinese Academy of Sciences (CAS), Beijing, 100101, China

ARTICLE INFO

Article history:
Received 11 October 2021
Received in revised form
27 February 2022
Accepted 28 February 2022
Available online xxx

Handling Editor: P Rioual

Keywords:
Peatland carbon cycle
Seasonality of warming
Anthropogenic warming
Historical natural warmings
Carbon-climate feedback

ABSTRACT

Peatland carbon accumulation generally increased during past intervals of natural warming. With recent anthropogenically-dominated warming being unprecedented over the past ~2000 years, however, it is unclear how peatland carbon dynamics may operate compared to those under historical natural warmings. Here we examine the impacts of the recent warming from 1850 CE to present (Recent Warm Period; RWP) and the historical warming during 1000–1300 CE (Medieval Warm Period; MWP) on peatland carbon accumulation of the Tibetan Plateau using two continuous peat core records. We observed major seasonal difference between the two warming periods, with growing season (summer) warming dominating the MWP, while greater non-growing season warming characterizing the RWP. Consequently, we found a high net carbon balance during the MWP, suggesting that warming increased plant production more than decomposition of organic matter. In contrast, a low net carbon balance was observed during the RWP because non-growing season warming greatly enhanced soil carbon decomposition that could have completely offset plant carbon uptake. Therefore, recent anthropogenic warming might have induced a different ecosystem response with lower net carbon balance over the past millennium than that during historical natural warmings. As other regions of the globe have similar growing season versus non-growing season warming patterns, the risk of carbon loss from global peatlands may have been underestimated, implying that there is an even greater challenge for managing ecosystem carbon sinks under future climate change.

1. Introduction

Peatlands contain one-third of the global soil carbon storage (Gorham, 1991; Yu et al., 2010) and thus they play a critical role in the global carbon cycle and climate change feedbacks (Joosten et al.,

* Corresponding author. State Key Laboratory of Tibetan Plateau Earth System Science (LATPES), Institute of Tibetan Plateau Research, Chinese Academy of Sciences, Beijing, 100101, China.
E-mail address: jbliu@itpcas.ac.cn (J. Liu).
[1] These authors contributed equally to this work.

https://doi.org/10.1016/j.quascirev.2022.107449
0277-3791/

2016; Leifeld and Menichetti, 2018). However, the response of the peatland carbon cycle to climate change is still poorly understood, making it a major source of uncertainty in climate projections (IPCC, 2014). During climatic warming, changes in peatland carbon stocks are governed by two opposing processes. In one process, warming enhances plant growth, which provides increased input to peat carbon accumulation via plant litter; and in an opposing process, warming also accelerates soil carbon loss via microbial respiration of plant litter and soil carbon (Friedlingstein et al., 2006). The overall net impact of warming on carbon accumulation, including both its sign and sensitivity, remains largely unclear (Gallego-Sala et al., 2018; Morris et al., 2018; Wilson et al., 2016). Furthermore, changes in precipitation and evapotranspiration would also influence the hydrologic regime, microbial decomposition, and carbon accumulation of peatlands.

Dated soil cores provide valuable information for understanding peatland carbon accumulation dynamics in response to temperature anomalies (Loisel et al., 2014). Almost all previous studies have indicated increased peatland carbon accumulation and expansion during past warm periods, on a large spatial scale: northern peatlands (Charman et al., 2013; Yu et al., 2010), to peatlands at regional scale in Western Siberia (Smith et al., 2004), Alaska (Jones and Yu, 2010), South America (Loisel and Yu, 2013a), and northern China (Wang et al., 2014b; Zhao et al., 2014). However, compared to past warm periods, the recent anthropogenic warm period may be characterized by a different warming pattern, with a higher warming rate at nighttime than during daytime, and a higher rate during the non-growing season than during the growing season (Davy et al., 2017; Hansen et al., 2010). Given the specific climatic characteristics of recent anthropogenic warming, however, it is unclear if the enhanced peatland carbon accumulation observed in past warm periods will also apply to continued anthropogenic warming.

Peatlands are also widely distributed across high mountains and plateaus where climate warming tends to be amplified; however, few studies have investigated the carbon accumulation patterns of these high-altitude peatlands. On the Tibetan Plateau, which has largest area of intact alpine peatlands on Earth, and where direct human disturbances are relatively minor compared to more populated regions, the recent anthropogenic warming rate is more than twice the global average (Yao et al., 2019). Thus, the Tibetan Plateau is well suited to an investigation of the peatland carbon cycle response to recent (anthropogenically dominated) and past (natural) warmings.

In contrast to warming episodes over the past millennia that were driven by natural climatic variations (Liu et al., 2013), recent warming is caused mainly by anthropogenic greenhouse gas emissions. This recent warming is also unprecedented in magnitude over the past 2000 years (IPCC, 2013; Neukom et al., 2019; Schurer et al., 2017), and in addition it has complex interactions with multiple anthropogenic forcing factors (Chen et al., 2021). Therefore, it is an intriguing question whether peatland soil carbon dynamics under recent warming conditions may differ from those of the past. Understanding the differences and similarities between past and recent warmings, in terms of soil carbon dynamics in peatlands and the underlying climatic drivers, will provide important information for predicting future changes in peatland carbon storage under future climatic change scenarios. Northern Hemisphere climate evolution over the past millennium could be divided into three major episodes: "Medieval Warm Period" (MWP), "Little Ice Age" (LIA), and "Recent Warm Period" (RWP) (Liu et al., 2013). The MWP is confirmed to be driven by natural climatic factors (Liu et al., 2013), which is the closest to those of the modern period and was thus often used as a paleoclimatic analog for long-term climate prediction (Liu et al., 2013).

In order to compare the carbon dynamics of these two warm climate periods, it is necessary to model the past changes in the net carbon balance of peatlands (Young et al., 2021). Conceptual and process models of peatland development have been produced for understanding carbon accumulation and carbon stocks. The Clymo bog growth model (BGM) assumes that the litter production rate and decomposition coefficient are constant. Although the Clymo's BGM model does not take account of some hydrological linkages and has some limits, this model can be used to derive peat-addition rate and peat decomposition rate from the cumulative carbon pool data to understand the long-term overall peat accumulation dynamics (Yu, 2011). The Holocene Peat Model (HPM) of Frolking et al. (2010) contains the hydrological influences and feedbacks. This model uses 12 plant functional types (PFTs) to represent peatland vegetation, with each PFT having different litter production and decomposition characteristics. Even so, this model still cannot reproduce the detail of variation in peat properties in the core. The Land surface Processes and eXchanges model (LPX) features a dynamic nitrogen cycle, a dynamic carbon transfer between peatland acrotelm and catotelm, hydrology and temperature dependent respiration rates, and peatland specific PFTs (Spahni et al., 2013). The LPX does not take the spatial scale, and effect of spatial differences into account. Baird et al. (2012) produced a 3-dimensional (3D) model (DigiBog) that treats peatlands as complex and adaptive and that allows for hydrological feedbacks across a range of spatial scales. Both DigiBog and HPM are process models, which have been used to understand the behavior of real-world systems through changing certain parameters over time (Yu et al., 2001). However, these models require several parameters that are not readily available for our study region. As the models are updated, these models are getting closer and closer to the actual development of peatlands. In this way, we can use these models under certain assumptions and the observed data to reconstruct past changes in the net carbon balance.

Here we use well-dated, high-resolution net carbon balance records from two alpine peatlands from hydrologically-closed basins in the Tibetan Plateau, the world's highest landmass. Our aims were to investigate and compare the responses of peatland soil carbon accumulation during a natural warming episode of the past millennium and those during recent anthropogenic warming. We found significant differences in seasonal climate signatures, and thus in soil net carbon balance between the two periods. In contrast to past natural warming when much of the warming occurred during the growing season, anthropogenic warming was particularly faster during the non-growing season, which reduced the net carbon balance of the Tibetan Plateau peatlands because non-growing season warming greatly enhanced soil carbon decomposition that could have wholly offset plant carbon uptake. Hence the risk of carbon loss from the world's peatlands may have been underestimated because other regions of the globe have similar growing season versus non-growing season warming patterns.

2. Methods

2.1. Study sites and sediment archives

The Tibetan Plateau and its surroundings comprise the Earth's largest mountain mass, with an average elevation exceeding 4000 m above sea level (m a.s.l.) (Fig. 1). The warming rate of the region over the last half century is more than twice the global average (Kuang and Jiao, 2016) and the Tibetan Plateau has the largest area of the world's highland peatlands (Yu et al., 2010). We selected two peatlands located in hydrologically-closed basins and geographically separated by ~300 km: Galang Co (GLC) (29°54′N, 95°36′E; 2821 m a.s.l) and Zhenbu Co (ZBC) (29°40′N, 92°23′E;

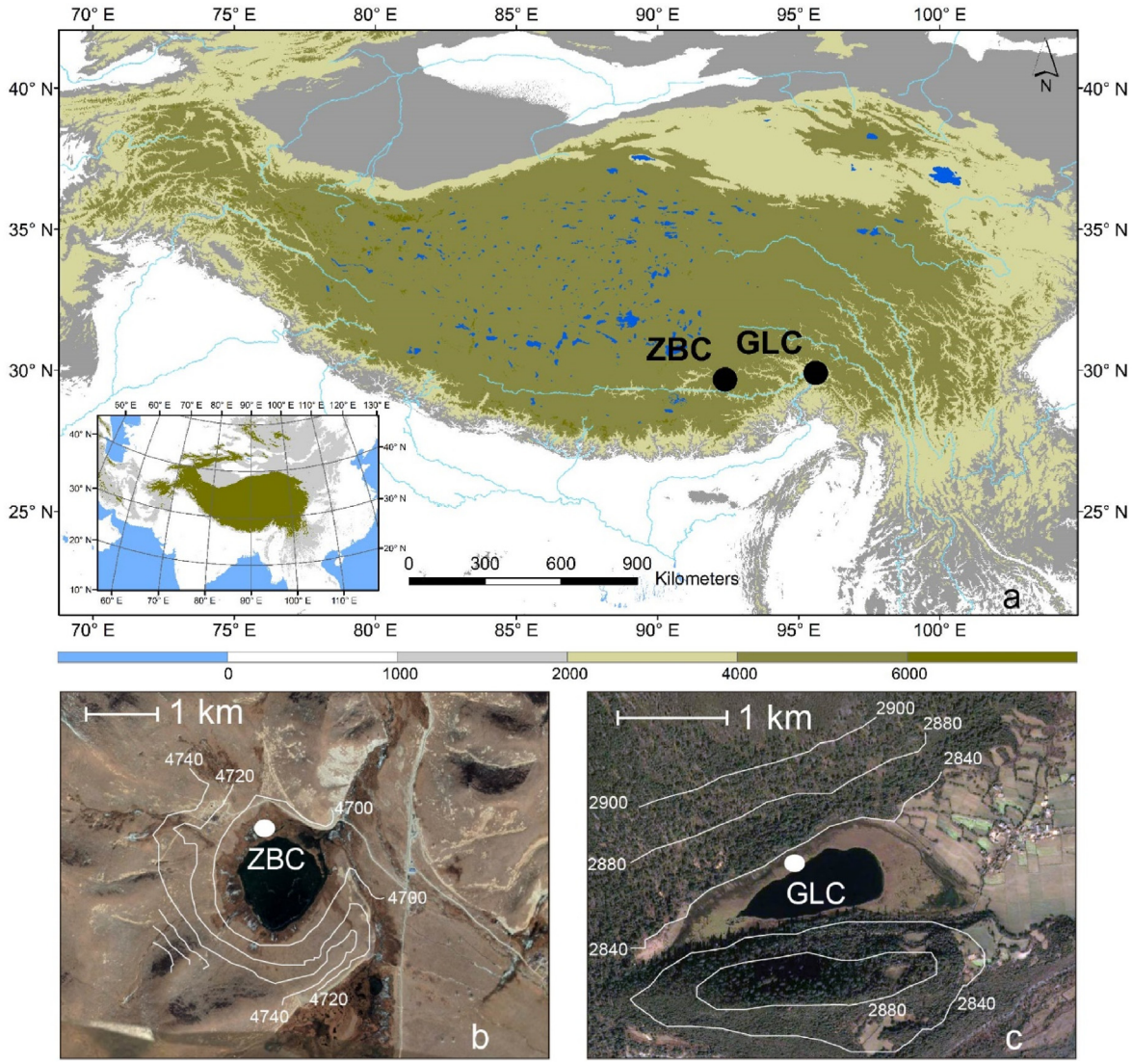

Fig. 1. Peat records from the Tibetan Plateau. (a) Elevation map of the Tibetan Plateau showing locations of the study sites (GLC and ZBC peatlands). Lakes are indicated by blue shading and major rivers by light-blue lines. The colors represent elevations (m a.s.l.) as shown in the color bars below. The two sites are separated by ~300 km with an elevation difference of ~1800 m. (b–c) Satellite images of the ZBC and GLC peatlands (source from Google Earth). White lines are contours. (For interpretation of the references to color in this figure legend, the reader is referred to the Web version of this article.)

4677 m a.s.l.) (Fig. 1). The two peatlands also have a more than 1800 m elevation difference and consequently they differ in mean annual temperature (8.9 °C at GLC vs. 6.4 °C at ZBC). Both sites are pristine and the vegetation is currently dominated by *Kobresia* and *Carex* plants (Supplementary Fig. S1).

We collected two peat cores from the GLC and ZBC peatlands in September 2019 using a Russian peat corer (Fig. 1). Both cores spanned the entire interval of peat accumulation, with the bases of the cores reaching the underlying clay and silt deposits (Fig. 2). The length of peat core GLC was 93 cm and that of core ZBC was 80 cm. The cores were sub-sampled at 1-cm intervals, but here we only focus on the peat sediments above the silty clay sediments. The chronology was established using accelerator mass spectrometry (AMS) ^{14}C dating of seven terrestrial plant macrofossils samples (which are unaffected by the reservoir effect) and one bulk organic sediment sample. Radiocarbon analysis was carried out at Beta Analytic Laboratory and ^{14}C Chronology Laboratory of Lanzhou University using AMS. The measured and calibrated ages are listed in Table 1. The ages are expressed in years before present (BP), where "present" is defined as 1950 CE (Common Era). Bayesian age-depth modelling (Bacon) was performed using OxCal v4.2.2 and a Poisson-process (P-sequence) single depositional model at 1-cm increments, with a K value of 100 (Blaauw and Christen, 2011; Ramsey, 2008), to produce the age-depth model (Fig. 2).

2.2. Acrotelm/catotelm boundary detection

To quantify and compare decadal and centurial-scale carbon accumulation rates, the acrotelm/catotelm boundary need to be identified (Loisel and Yu, 2013b). As plant litter and new peats in the acrotelm are exposed to oxygen, they are subjected to a higher decay rate. Once in the catotelm, the decay rate declines and becomes slower under anaerobic conditions. Therefore, the long-term maximal depth of the summer water table, reflecting the maximum depth of oxygenated conditions, is usually used to define the acrotelm/catotelm boundary (Ingram, 1982). We measured the water level in a steady state with a meter ruler after we drilled the peat core. The ratio of precipitation to temperature that affects the

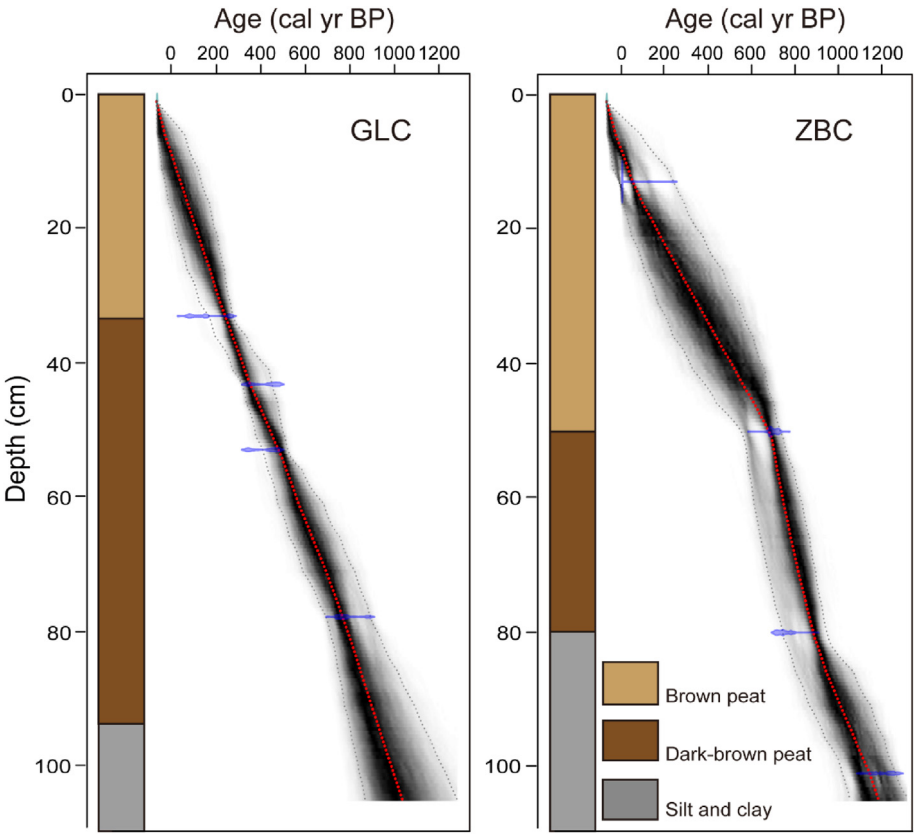

Fig. 2. Lithostratigraphy and Bacon age-depth models for the GLC and ZBC peat cores. The different colors of the rectangular column represent changes in lithology. The transparent light blues are the calibrated ^{14}C dates, and the darker greys indicate the most probable calendar ages. The grey stippled lines are 95% confidence intervals and the red curve is the single 'best' model based on the median age for each depth interval. (For interpretation of the references to color in this figure legend, the reader is referred to the Web version of this article.)

Table 1
Results of AMS ^{14}C dating analysis of the GLC and ZBC peat cores from the Tibetan Plateau.

Laboratory number	Core ID	Depth (cm)	Analyzed material	Conventional radiocarbon age (yr ^{14}C BP)	$\delta^{13}C$ (‰)	Calibrated age (cal yr BP, 2σ range)
Beta544060	GLC-33	32–33	Stem	80 ± 30	−27.0	105 (24–260)
Beta 558954	GLC-43	42–43	Stem	380 ± 30	−23.6	449 (318–505)
Beta 544068	GLC-53	52–53	Stem	410 ± 30	−27.9	483 (367–520)
Beta 544061	GLC-78	77–78	Stem	880 ± 30	−27.5	788 (728–908)
LZU20090	ZBC-13	12–13	Stem	10 ± 20	−24.4	51 (40–240)
Beta544063	ZBC-50	49–50	Stem	760 ± 30	−26.6	691 (666–730)
Beta 544064	ZBC-80	79–80	Stem	830 ± 30	−25.7	887 (744–1087)
Beta 544067	ZBC-101	100–101	OS	2050 ± 30	−26.0	1223 (1130–1315)

Note that all of the dated materials are terrestrial plant macrofossils, except for sample 544067 from the ZBC peat core, which was bulk organic sediment. Linear extrapolation method was used to measure the reservoir effect on radiocarbon ages of sample 544067 from the ZBC peat core. The calculated reservoir age is ~800 years, which is consistent with reservoir ages estimated from the Tibetan Plateau (Hou et al., 2012). The chronology was established using accelerator mass spectrometry (AMS) ^{14}C dating of seven terrestrial plant macrofossils that were unaffected by the reservoir effect, and one organic sediment (OS) sample.

water level of peatlands in the summer of 2019 was almost the average value in recent decades in GLC and ZBC (Supplementary Fig. S2). Therefore, the measurement of water table position in September 2019 could be seen as a good approximation of the acrotelm/catotelm boundary.

2.3. Peat property and macrofossil analysis

Volumetric peat samples were freeze-dried for 12 h to determine the dry bulk density (DBD). The organic carbon (OC) content was determined using a total organic carbon analyzer (TOC-5000A, Shimadzu). On the basis of the chronologies and the measured DBD (g cm^{-3}) and organic matter content (OM, %; OC × 2), we can calculate the cumulative peat (M) data.

Peat sub-samples were washed with a strong jet of water over a 125 μm sieve after estimating the abundance of unidentifiable organic matter (UOM). The residues were inspected under a stereo microscope at 7.3 × to 120 × magnification, and 400 × magnification when necessary. The relative abundance of plant species at each depth interval was estimated using a 10 × 10 square grid salver.

2.4. Conceptual peatland carbon accumulation modeling

The basal layers of the peat cores have undergone decomposition for a longer time than the upper layers, so we used the

conceptual model of Clymo (1984) to represent this autogenic peat accumulation process. Assuming a constant peat addition rate (PAR; g OM m^{-2} yr^{-1}) driven by plant NPP at the top of the peat column, and a constant peat decay coefficient (α; yr^{-1}), the PAR and α were derived directly from the cumulative peat data for the acrotelm and catotelm separately by using the Clymo's model (Supplementary Fig. S3):

$$M = \frac{PAR}{\alpha} \times (1 - e^{-\alpha t}) \quad (1)$$

where M is the cumulative peat (g cm^{-2}) at time t (yr). The PAR determines the general slope of the cumulative peat versus age curve, and α determines the curvature (Yu et al., 2003).

The PAR and α of each peat core were evaluated using a curve-fitting procedure. The modeled decay coefficient values were then used to reconstruct the peatland carbon fluxes using the empirical model of Yu (2011). The Yu's peatland carbon flux reconstruction model uses the observed net peat carbon pool (NCP) values obtained from peat cores to back-calculate net carbon uptake (NCU) by considering NCU as the initial input of peat carbon. The net carbon release (NCR) represents the summed carbon release of all peat cohorts. Both NCU and NCR take into account changing plant production inputs, despite being derived from a constant decay constant. Time histories of peat carbon uptake and release were divided at 10-year intervals. The equations of the Yu's model have the following form:

$$NCU_t = \frac{NCP_t}{e^{-\alpha * t}} \quad (2)$$

$$NCR_t = \sum_{k=t}^{initiation\ age} \left(\frac{NCP_k}{e^{-\alpha * t}} - \frac{NCP_k}{e^{-\alpha * (t-1)}} \right) \quad (3)$$

where k is the peat cohort ID to track all peat cohorts older than time t since the peatland initiation. For example, $k = 1$ means the peat cohort of the last 10 years. The net carbon balance (NCB) was calculated as the difference between NCU and NCR as derived above,

$$NCB = NCU - NCR \quad (4)$$

The Frolking's peat decomposition model (Frolking et al., 2001) was used to simulate the amount of peat transferred from the acrotelm to the catotelm. The equation has the following form:

$$M_t = \frac{PAR}{1 + \alpha t} \quad (5)$$

where PAR is the constant rate of organic matter added to the acrotelm, and a small amount of peat is transferred into the catotelm (M_t) after decomposition (α) over time t. Thus, this approach links the acrotelm peat carbon fluxes to the long-term rate of peat storage by comparing remaining acrotelm peat mass at the acrotelm/catotelm boundary to the catotelm peat input term (Loisel and Yu, 2013b). After a period of time, how much peat carbon in the current acrotelm will be transferred into the catotelm following aerobic decay is predicted and this value can be compared with the long-term peat carbon pool.

2.5. Statistical analysis of meteorological data to determine temperature trends

We obtained daily surface temperature data from the China Meteorological Data Service Center. The data are subjected to rigorous quality control by the China Meteorological Administration to ensure their quality and integrity, via inspection of the format, missing values, limit values, changes in range, internal consistency, and spatiotemporal consistency. The 94 meteorological stations on the Tibetan Plateau and the surrounding region with an elevation higher than 2000 m a.s.l. were selected in this study. Detailed information about the meteorological stations is given in the Table S1. Amongst these 94 stations, Xiangride and Maqing have been updated to December 1997. Monthly mean surface temperature is calculated if the specified month has more than 24 days using daily mean surface air temperature data. The regional average values for Tibetan Plateau are derived from the average of all 94 stations for the period (until 2019).

3. Results

3.1. Core chronology

The 93-cm long peat core GLC has an age of 728–908 cal yr BP at the depth of 78 cm, and the 80-cm long peat core ZBC has a basal age of 744–1087 cal yr BP (Table 1), based on Bacon age modeling results (Fig. 2). The youngest ^{14}C data of the GLC is 24–260 cal yr BP (33 cm), and the youngest ^{14}C data of the ZBC is 40–240 cal yr BP (13 cm). For each peat core the Bacon model was used to construct a chronological frame spanning the past ~1000 years and based on four ^{14}C dates.

3.2. Peat geochemical properties

Based on the field observations of the long-term maximal depth of the summer water table, the acrotelm/catotelm boundary of GLC and ZBC are 8–9 cm and 5–6 cm deep, respectively. OC and DBD showed opposite trends, with the increasing OC and decreasing DBD from the bottom to the surface in GLC and ZBC peatlands (Supplementary Fig. S4). The average OC of GLC was 31%, and the average OC of ZBC was 24%. While the average DBD of the two peat cores was the same (0.04 g cm^{-3}). The average DBD of acrotelm samples (0.02 g cm^{-3}) was half less than that of catotelm samples (0.04 g cm^{-3}) for core GLC, and the average DBD of acrotelm samples (0.006 g cm^{-3}) was much lower than that of catotelm samples (0.04 g cm^{-3}) for core ZBC. The average carbon density values of GLC and ZBC are 0.011 and 0.007 g C cm^{-3}, respectively.

3.3. Modeled peat addition and decomposition patterns

Peat mass is the amount of peat per unit area. The cumulative peat mass of the 70 years (acrotelm) for GLC was 0.16 g OM cm^{-2}, and the cumulative peat mass of the 40 years (acrotelm) for ZBC was 0.03 g OM cm^{-2} (Fig. 3), while the cumulative peat mass of the previous 1000 years (catotelm) for GLC was 2 g OM cm^{-2}, and the cumulative peat mass of the 1000 years (catotelm) for ZBC was 1.1 g OM cm^{-2}. The PAR values of the acrotelm (29 ± 2 g OM $m^{-2}yr^{-1}$) and catotelm (28 ± 2 g OM $m^{-2}yr^{-1}$) for GLC were almost the same, and the PAR of acrotelm (9 ± 1 g OM $m^{-2}yr^{-1}$) for ZBC was much lower than that of catotelm (16 ± 2; 30 ± 3 g OM $m^{-2}yr^{-1}$). The decay coefficient (α) of the acrotelm (0.01 yr^{-1}) was higher than catotelm (0.001 yr^{-1}) for both GLC and ZBC cores.

The peatland carbon flux reconstruction model yielded NCU values for the catotelm that ranged between 7.1 and 37.4 g C $m^{-2}yr^{-1}$ in GLC, and the NCU values in ZBC ranged between 2.0 and 38.9 g C $m^{-2}yr^{-1}$ (Fig. 4). The summed carbon release of all peat cohorts was 16.1 g C $m^{-2}yr^{-1}$ in GLC, and 10.2 g C $m^{-2}yr^{-1}$ in ZBC. The peat decomposition model simulated peat mass loss in the acrotelm for 70 years in GLC, and for 40 years in ZBC. Remaining peat masses of 26 g m^{-2} after 10 years (equivalent to 89.7% of initial

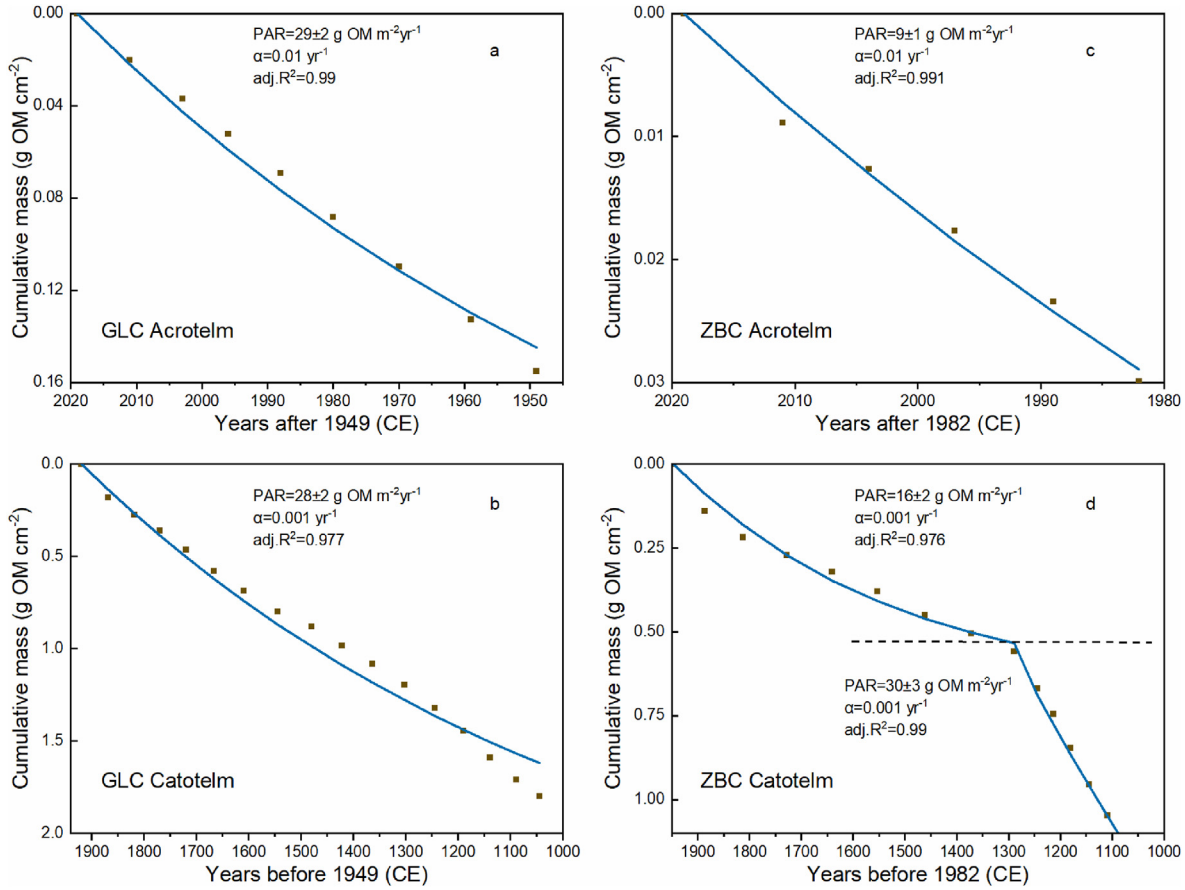

Fig. 3. Cumulative peat mass and exponential decay model for the GLC and ZBC peat cores. Peat accumulation patterns for GLC acrotelm (a), GLC catotelm (b), ZBC acrotelm (c), and ZBC catotelm (d). The brown dots represent the cumulative peat mass during different years, and the dark blue lines are the results of the fitted model. The dash line separates the two fitted models. (For interpretation of the references to color in this figure legend, the reader is referred to the Web version of this article.)

mass), and 16 g m^{-2} after 70 years (equivalent to 55.2% of initial mass) were obtained in GLC. Remaining peat masses of 8 g m^{-2} after 10 years (equivalent to 88.9% of initial mass), and 6 g m^{-2} after 40 years (equivalent to 66.7% of initial mass) were obtained in ZBC. The entire record can be divided into three periods: ~1000–1300 CE, ~1300–1850 CE and ~1850 CE to the present, which correspond respectively to the MWP, LIA, and RWP (Moberg et al., 2005) (Fig. 5a). For GLC, the average NCB values for the MWP, LIA and RWP are 22.7 ± 6.1, 2.15 ± 4, and −5.5 ± 1.5 g C $m^{-2}yr^{-1}$, respectively (Fig. 4b); and for ZBC they are 23.1 ± 10.6, −2.8 ± 2.1, and −4.2 ± 1.9 g C m^{-2} yr^{-1}, respectively (Fig. 4d).

3.4. Past vegetation change

Macrofossil records for cores GLC and ZBC (Supplementary Fig. S5) show that peat profiles have been always dominated by *Carex* and *Kobresia* throughout the last 1000 years. The *Carex* was abundant in presence with average levels of 18% and 26% in GLC and ZBC, respectively. The *Kobresia* remnants had averages of 36% and 40% in GLC and ZBC, respectively. There was more moss found in GLC than ZBC, and no *Potentilla* found in ZBC. The abundances of *Cynoglossum* in GLC and ZBC varied greatly, from absence to 63%. A few *Primula* leaves and stems were found in both cores GLC and ZBC.

4. Discussion

4.1. Tibetan Plateau peatlands development over the past millennium

The carbon accumulation records show clear multi-centennial-scale changes over the past millennium (Fig. 5b and c). NCU and NCB showed decreasing trends in both peatlands from ~1000 CE to the present (Fig. 5b and c). Therefore, even though both the MWP and RWP were/are anomalously warm, their net carbon accumulation balances are substantially different.

Precipitation were the primary sources of water input for the GLC peatland, and there was no glacial meltwater input over the past millennium (Zhou et al., 2010). For the ZBC peatland, current water sources were also dominated by precipitation, and no glaciers are currently present within its catchment; however, we cannot exclude the possibility that a glacier existed in the catchment during the MWP and LIA. Nonetheless, the consistent patterns of higher carbon accumulation during the MWP and lower carbon accumulation during the RWP for the two peatlands indicate that glaciers, if present, had minimal impact on peat carbon accumulation at the two sites over the past millennium. Neither GLC nor ZBC has runoff input, and their water source is ultimately precipitation to the peatlands or the small watersheds. Even if the water level in peatlands is influenced by lake level, the lake level likely reflects regional moisture balance and regional climate because of a very small watershed. The effective moisture record from regional studies (Yang et al., 2014) shows no obvious evidence

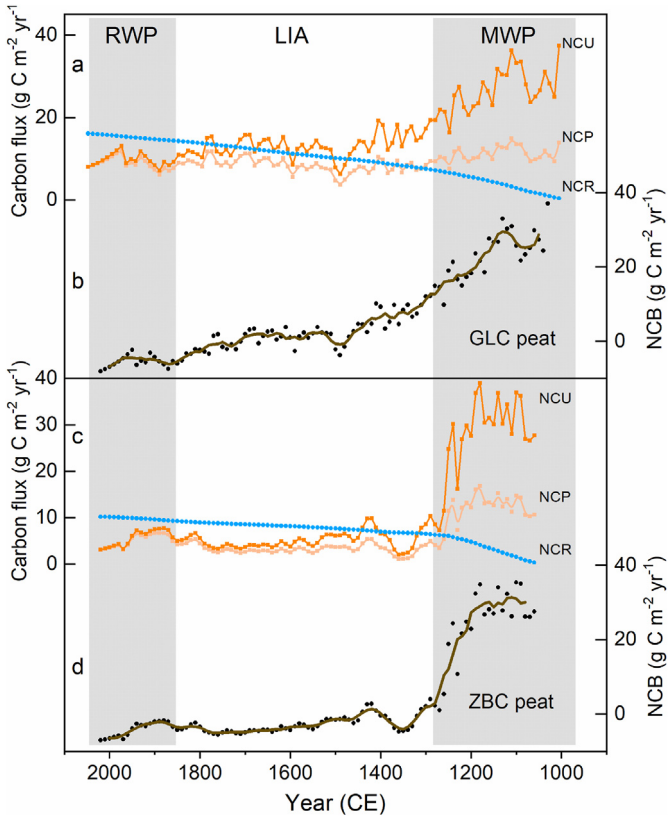

Fig. 4. Last millennium peat carbon fluxes for the GLC (a, b) and ZBC (c, d) peat cores using the empirical model of peatland carbon flux reconstructions of Yu (2011). The net carbon pool (NCP) represents today's peat stock as observed/reconstructed from peat cores; the net carbon uptake (NCU) represents the average annual peat carbon flux that entered the peatland over the past 1000 years, and the net carbon release (NCR) represents the summed carbon release of all peat cohorts over time. The net carbon balance (NCB, black dots) was calculated as the difference between NCU and NCR. The smoothed lines are five-point moving averages (brown line). (For interpretation of the references to color in this figure legend, the reader is referred to the Web version of this article.)

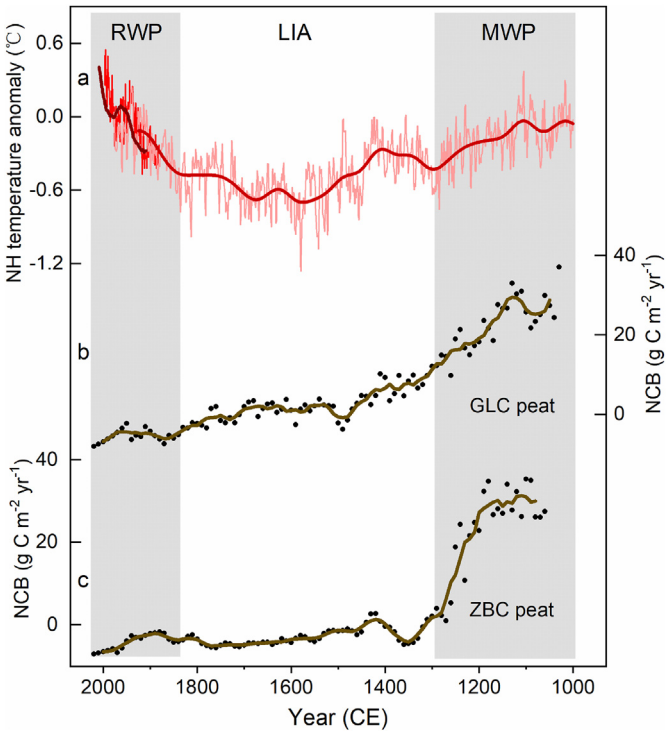

Fig. 5. Long-term trends in reconstructed net carbon balance (NCB) in the Tibetan Plateau peatlands compared with the Northern Hemisphere (NH) temperature anomaly over the past millennium. (a) Reconstructed NH mean temperature anomaly over the past millennium (Moberg et al., 2005) (light-red curve is the raw data and the dark-red curve is the 30-yr moving average), and NH mean temperature anomalies from 1850 CE to the present based on weather station data (red curve is the raw data and the black-red curve is the 30-yr moving average; ftp://ftp.ncdc.noaa.gov/pub/data/ghcn/v4). (b) Net carbon balance (NCB) in the GLC peatland (black dots). The brown fitted line is the result of five-point moving averages; (c) Net carbon balance (NCB) in the ZBC peatland (black dots). The brown fitted line is the result of five-point moving averages. Grey shading corresponds to the two warm periods recognized over the past millennium: the Medieval Warm Period (MWP) and the Recent Warm Period (RWP). (For interpretation of the references to color in this figure legend, the reader is referred to the Web version of this article.)

of the influence of lake level changes on carbon accumulation of the two peatlands over the past millennium (Supplementary Fig. S6), suggesting that the water level of the two hydrologically-closed peatlands was relatively stable. In the nearly 100 cm-long section of the two peatlands, we observed that minerals are mainly clay. The nutrient content of clay minerals is low compared to less-weathered, phosphate and feldspar minerals (Kylander et al., 2018). Therefore, clay minerals input might not have significant impacts on the peatland vegetation growth and carbon accumulation due to low nutrient contents. The vegetation compositions of the two sites show little changes over the past millennium (Supplementary Fig. S5), which enables us to exclude the effects of changes in vegetation composition on organic matter production and decomposition that influence peat carbon accumulation.

The peatlands at both GLC and ZBC were first formed at ~1000 CE (Fig. 2), when the climate transitioned from a cool to a warm period, as documented by rapid tree growth in the region (Wang et al., 2014a). A review of paleoenvironmental changes across the Tibetan Plateau indicates that 800–1000 CE marks the transition between a cooling interval and a warm period. Two tree ring width data series from the southeastern Tibetan Plateau indicate faster tree growth from 900 to 1000 CE due to increasing temperature (Hao et al., 2020). Increasing temperatures also increase the length of the growing season, which is an important limiting factor for helophyte growth (Aaby and Tauber, 1975). In addition, the warm climate favored helophyte colonization of the lakeside area, enabling peat to form at the MWP.

The basal peat date from ZBC is younger than that from GLC, as is also the carbon accumulation history (Fig. 2), which indicate a delay in carbon sink development of ZBC core compared to GLC. The meteorological data from the nearby weather stations show that the annual temperature in the GLC peatland (8.9 °C) is greater than at the ZBC peatland (6.4 °C) due to the lower altitude; therefore, the temperature of GLC was generally always higher than at ZBC over the past millennium. Higher temperatures promoted earlier helophyte growth in the lakeside area of GLC than at ZBC, and the temperature differences in the growing seasons may have caused a 50-year delay in peat initiation at the ZBC peatland. This evidence supports the positive relationship between peatland carbon accumulation and temperature during the MWP. Therefore, the differences in the timing of peat formation between the two peatlands were mainly due to temperature differences (that is, because the ZBC peatland is at a lower elevation than GLC).

4.2. *Different carbon-climate feedbacks under past and recent warming*

The MWP and RWP were the two most important warming

intervals over the past millennium (Liu et al., 2013) (Fig. 5a). The MWP warming was driven by natural climatic factors, while that of the RWP is driven mainly by anthropogenic greenhouse gas emissions (Liu et al., 2013). Using mean annual temperature record reconstructed from four ice cores from across the Tibetan Plateau (Yao et al., 2019) (Fig. 6d), and summer temperature anomalies reconstructed from sediment alkenone measurements at three lake sites (Fig. 6b; see Supplementary Fig. S7), we found that the mean annual temperature during the MWP was the lowest over the past millennium, but that the summer (growing season) temperature was the highest. This implies that the MWP warming in the Tibetan Plateau occurred mainly in summer, and its non-growing season temperature increase was small compared to that of the RWP. During the RWP, the summer temperature was lower than that of the MWP (Fig. 6b), while the mean annual temperature was the highest over the entire last millennium (Yao et al., 2019) (Fig. 6d). Hence, warming during the RWP can be mainly attributed to the non-growing season temperature, with the temperature increase of the growing season being less than that of the MWP. Records of monthly temperature for the six most recent decades averaged across the 94 meteorological stations in the Tibetan Plateau also confirm a much larger increase in non-growing season temperatures (0.46 °C per decade in the winter months, DJF) compared to those of the growing season (0.21 °C per decade in the summer months, JJA) (Fig. 7). Therefore, the seasonal warming pattern during the RWP is different from that recorded during the MWP, which was forced by natural factors.

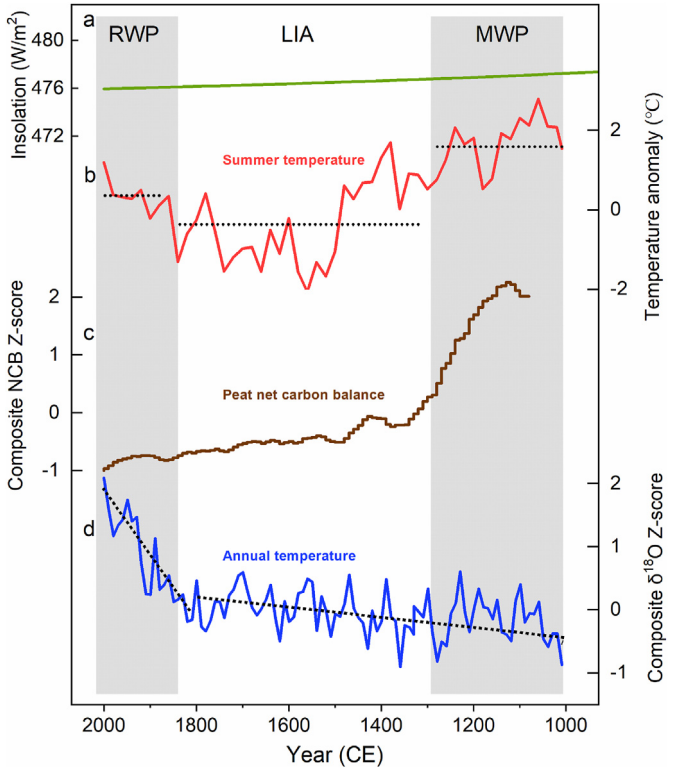

Fig. 6. Comparison of the net carbon balance (NCB) over the past millennium in peatlands of the Tibetan Plateau with natural and anthropogenic forcings. (a) Northern Hemisphere summer insolation curve (Berger and Loutre, 1991). (b) Tibetan Plateau summer (growing season) temperature anomaly over the past millennium integrated from three alkenone-based summer temperature records (He et al., 2013; see supplementary Fig. S7 for detail). (c) 10-year bins of Z-scores of composite NCB of the GLC and ZBC peatlands (this study). (d) Tibetan Plateau mean annual temperature curve over the past millennium reconstructed from the composite of four ice core $\delta^{18}O$ records from across the Tibetan Plateau (Yao et al., 2019). Dashed lines in (b) and (d) represent periods of different change rates. Grey shading corresponds to the two warm periods recognized over the past millennium: the Medieval Warm Period (MWP) and the Recent Warm Period (RWP).

We then calculated the average values of the 10-year interpolated Z-scores of the NCB for each peat core (GLC and ZBC) (Fig. 6c), which showed that higher NCB corresponded to a greater magnitude of warming during the growing season (Fig. 6b), but a lesser degree of warming during the non-growing season (as inferred from the relationship between Fig. 6b and d) in the MWP, with almost no change in summer solar insolation (Berger and Loutre, 1991) (Fig. 6a). The greater growing season warming during the MWP would have promoted increases in net primary productivity by extending the length of the growing season and enhancing plant growth. While microbial activity and peat decomposition would also have been higher during the growing season, they would be largely unchanged during the non-growing season due to the lesser degree of warming during that season (Yu et al., 2010). Therefore, during the MWP, the increase in the plant NPP rate was higher than the increased microbial respiration rate, leading to the formation of peat and increased net peat carbon balance in the Tibetan Plateau (Fig. 6c). This high net carbon accumulation balance under natural warming provided negative feedback to climatic warming (Fig. 8).

In contrast to the MWP, the lower NCB during the RWP (Fig. 6c) corresponded to a lesser degree of warming during the growing season (Fig. 6b) and greater warming during the non-growing season (as inferred from the relationship between Fig. 6a and d), with almost no change in summer insolation (Fig. 6a). The lesser degree of warming in the growing season would have limited the increase in NPP via shortening the length of the growing season and thereby limiting plant growth. In addition, the greater warming during the non-growing season would accelerate microbial activity and peat decomposition. The increased soil organic carbon decomposition during the non-growing season was so great that it exceeded the increased rate of growing season NPP. As a result, the Tibetan Plateau peatlands during the RWP were actually a poor carbon sink or even an atmospheric carbon source (Fig. 6c), which further provided a positive carbon accumulation - climate warming feedback (Fig. 8). Hence, the net carbon balance during the recent anthropogenically-dominated warming was the lowest in the past millennium and its variation exceeded natural variability (Fig. 6c).

Although rising atmospheric temperatures could influence the length of the growing season and plant growth, a snow cover could have an insulating effect in the winter, keeping soil temperatures slightly warmer and thus leading to faster decomposition. As greater non-growing season warming characterizes the RWP and warmer air can hold more moisture, the snow cover on the Tibetan Plateau should have increased in RWP. Indeed, the snow mass over the Tibetan Plateau has increased with increasing air temperature based on the microwave satellite remote-sensing data (from 1978 to 2006) and meteorological observation data (Che et al., 2008). As snow thickness increases, the insulating effect of snow cover increases and results in a warmer soil. Warmer soil temperature would increase peat decomposition and result in low carbon accumulation. The insulating effect reaches the maximum when snow is at its optimal thickness (about 40 cm), and the average snow-depth of the two sites is 7–9 cm from 1978 to 2006 during winter (Che et al., 2008). The depth of snow cover in the MWP might be lower than 7–9 cm. Therefore, further increase in snow thickness would increase insolation effect, causing soil warming, elevated decomposition, and reduction in carbon accumulation. On the other hand, the MWP warming in the Tibetan Plateau occurred mainly in summer, and its non-growing season temperature increase was minimal compared to that of the RWP. Therefore, the snow cover of the two sites was fragile, and the snow cover may have had less insulating effect on soil temperature in the MWP.

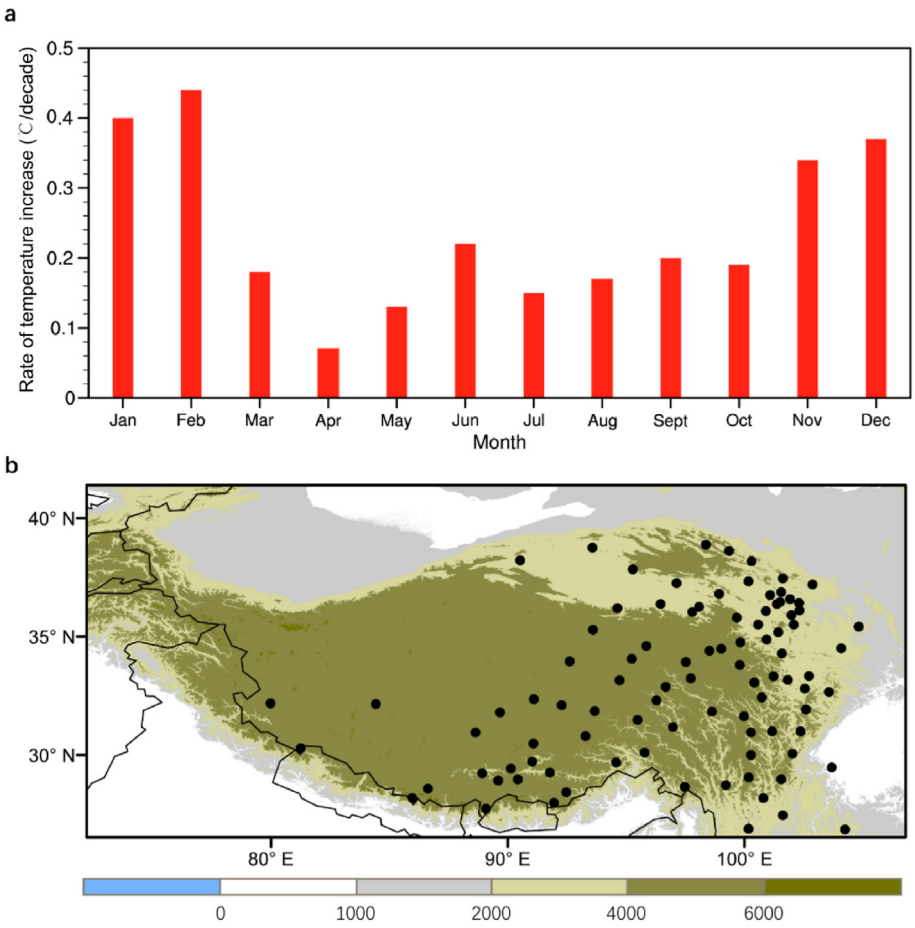

Fig. 7. Rate of monthly mean temperature increase at elevations above 2000 m a.s.l. on the Tibetan Plateau. (a) The statistics of the rate of monthly temperature increase averaged over the 94 meteorological stations show that the warming over the last six decades mainly occurred in the non-growing season, especially in the winter season, and that the temperature increment of the growing season (summer season) is small. (b) Locations of the meteorological stations above 2000 m a.s.l. in the Tibetan Plateau are indicated by black dots. Land topography information was obtained from the ETOPO1 dataset (Amante and Eakins, 2009). The color bars represent elevations in m above sea level (a.s.l.). (For interpretation of the references to color in this figure legend, the reader is referred to the Web version of this article.)

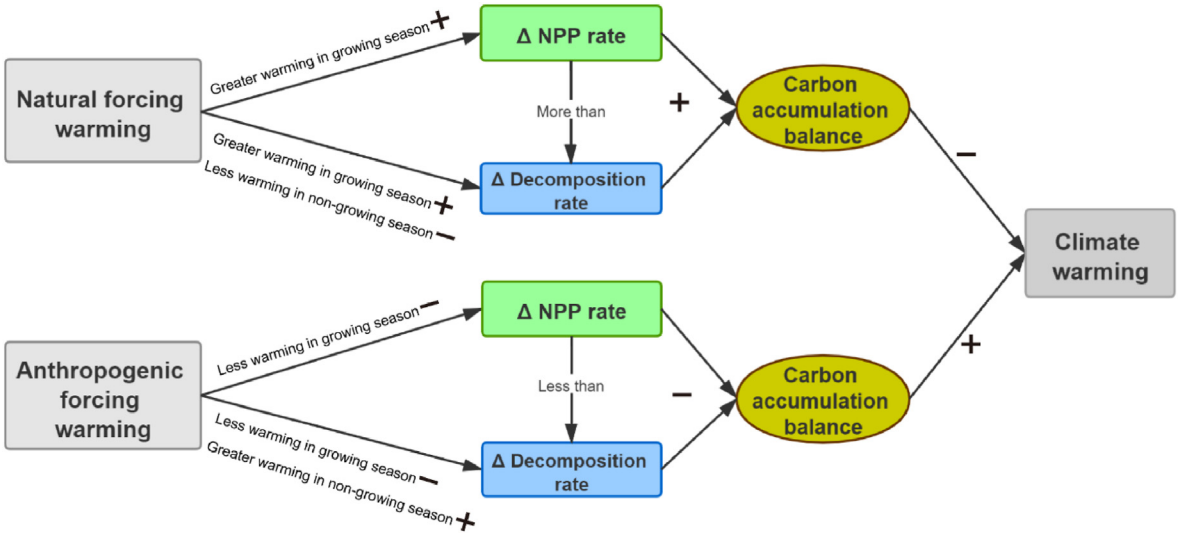

Fig. 8. Conceptual model of the peatland carbon-climate feedback for the Tibetan Plateau. Arrows represent effective processes, and the boxes represent different variables related to peat carbon accumulation. '+' and '-' indicate positive and negative feedback, respectively. △NPP rate represents an increased rate of NPP, and △Decomposition rate represents an increased rate of peat decomposition.

Indeed, our carbon flux measurement data also documented that the annual carbon emissions in the peatlands of the Tibetan

Plateau during the non-growing season were 2.4–4.1 times higher than those during the growing season (Supplementary Fig. S8). The net ecosystem carbon balance (NECB; Chapin et al., 2006) as often calculated from carbon flux measurements is similar to NCB conceptually (Yu, 2012), but they were derived differently. The NECB is often derived from direct measurements or calculations of various carbon flux terms explicitly, including net ecosystem production, calculated ecosystem respiration, CH_4 emissions and fluvial outputs of dissolved carbon. Due to spatial and time constraints, however, non-respiratory carbon release, such as from fires and volatile organic carbon, are often not included. On the other hand, the NCB is derived through decomposition of the observed final carbon accumulation values into two flux terms representing carbon uptake and carbon release—the latter implicitly including all carbon output fluxes as mentioned above. Both approached have respective pros and cons in terms of process understanding and timescales, and their further integration would advance ecosystem carbon cycle research, including understanding and projecting responses of terrestrial ecosystems to global change at relevant decadal and multidecadal timescales.

There are quite a few studies that show that the recent warming has led to a decline in carbon accumulation in peatlands in the pan-Arctic (Chaudhary et al., 2020), Minnesota (Hopple et al., 2020), and Finland (Zhang et al., 2020). These areas also showed greater non-growing season warming during the recent 50 years. Nevertheless, none of them proposed that the growing season versus non-growing season warming patterns play an important role in recent carbon release. Instead, they suggest that the permafrost thaw or the drought caused by warming is the leading cause of carbon release in peatlands. However, we believe that the greater non-growing season warming in recent anthropogenic warming is one of the critical reasons for the peatland carbon release. According to the IPCC Sixth Assessment Report (IPCC, 2021), other regions across the world show a similar pattern in warming seasonality, suggesting that the risk of carbon loss from the world's peatlands have been underestimated.

5. Conclusions and implications

It has been long recognized that climate change has important impacts on peatland carbon dynamics. Early studies have established a global relationship between peatland carbon accumulation rates and climate changes (Gallego-Sala et al., 2018). Extensive peat carbon accumulation during warmer periods is also recorded in northern peatlands through the last glacial cycle (Treat et al., 2019). However, no studies have thus far explicitly assessed the impacts of seasonal warming patterns on peat net carbon accumulation balance. Considering that carbon dynamics could vary significantly across different seasons, this lack of a seasonal warming pattern may be a major source of uncertainty in assessing the response of the global peatland carbon cycle to climate change.

The past can be used to generate scenarios for the future, and the peatland carbon cycle during past warm periods has often been used to predict its future trajectory under anthropogenic warming. However, for such projections, one needs to compare and validate if the recent and projected anthropogenic warming mimic the behaviors of past warmings, in particular in terms of the seasonality of warming. Such essential comparisons, however, are scarce in the literature. On the Tibetan Plateau, recent anthropogenic warming is generating a climate signature different from that of past warming driven by natural forcing. During the MWP, when the growing season dominated the warming, the Tibetan Plateau peatlands acted as a strong carbon sink, while during the RWP, with dominant non-growing season warming, they were a carbon source. This anthropogenic warming might have induced a different ecosystem response, with a large decrease in carbon sequestration.

We have reported results from two peatlands, and both sites are situated adjacent to lakes that may not be representative of "typical" northern peatlands. We argue that local hydrology of these peatlands likely reflects regional moisture balance due to their small watersheds, but further studies of oligotrophic or ombrotrophic bogs would be needed to confirm our findings. Furthermore, the magnitude of the changes reported in this study should be treated with caution when extrapolating to other sites or regions. In any case, our results provide one of the first tests of a critical hypothesis about the important role of climate seasonality in controlling long-term carbon accumulation in peatlands.

Data and code availability

The peat carbon accumulation data and R scripts used for post-processing data are available at: Dryad https://doi.org/10.5061/dryad.h70rxwdj7.

Credit author statement

Jianbao Liu: Conceptualization, Methodology, Validation, Formal analysis, writing-reviewing and editing, Visualization, Supervision, Project administration, Funding acquisition. **Hanxiang Liu:** Conceptualization, Methodology, Software, Validation, Formal analysis, Investigation, Resources, Data curation, Writing – original draft, writing-reviewing and editing, Visualization. **Huai Chen:** Resources, writing-reviewing and editing, Visualization. **Zicheng Yu:** Writing-reviewing and editing, Visualization. **Shilong Piao:** Writing-reviewing and editing, Visualization. **John P. Smol:** Writing-reviewing and editing, Visualization. **Jifeng Zhang:** Conceptualization, Investigation, Resources. **Lingxin Huang:** Methodology, Data curation, Writing – original draft. **Tao Wang:** Writing-reviewing and editing. **Bao Yang:** Conceptualization. **Yan Zhao:** Writing-reviewing and editing. **Fahu Chen:** Supervision, Project administration, Funding acquisition.

Declaration of competing interest

The authors declare that they have no known competing financial interests or personal relationships that could have appeared to influence the work reported in this paper.

Acknowledgements

We thank L.D. Tian and X. Zhang for helpful discussions; J. Chen, S.Q. Chen, H.H. Cao, and F.Y. Li for laboratory assistance; and four journal reviewers for critical and constructive comments that improved the manuscript. This work was supported by Basic Science Center for Tibetan Plateau Earth System (BSCTPES, NSFC project No. 41988101), the Second Tibetan Plateau Scientific Expedition and Research Program (STEP) (2019QZKK0601), Pan-Third Pole Environment Study for a Green Silk Road of CAS Strategic Priority Research Program (XDA20090000), and National Natural Science Foundation of China (42071115, 41790421, 42001081, 41877458).

Appendix A. Supplementary data

Supplementary data to this article can be found online at https://doi.org/10.1016/j.quascirev.2022.107449.

References

Aaby, B., Tauber, H., 1975. Rates of peat formation in relation to degree of

humification and local environment, as shown by studies of a raised bog in Deninark. Boreas 4, 1–17.
Amante, C., Eakins, B., 2009. ETOPO1 1 Arc-Minute Global Relief Model: Procedures, Data Sources and Analysis, NOAA Technical Memorandum NESDIS NGDC-24. National Geophysical Data Center, NOAA. https://doi.org/10.7289/V5C8276M.
Baird, A.J., Morris, P.J., Belyea, L.R., 2012. The DigiBog peatland development model 1: rationale, conceptual model, and hydrological basis. Ecohydrology 5, 242–255.
Berger, A., Loutre, M.F., 1991. Insolation values for the climate of the last 10 million years. Quat. Sci. Rev. 10, 297–317.
Blaauw, M., Christen, J.A., 2011. Flexible paleoclimate age-depth models using an autoregressive gamma process. Bayesian Anal. 6, 457–474.
Chapin, F.S., Woodwell, G.M., Randerson, J.T., Rastetter, E.B., Lovett, G.M., Baldocchi, D.D., Clark, D.A., Harmon, M.E., Schimel, D.S., Valentini, R., Wirth, C., Aber, J.D., Cole, J.J., Goulden, M.L., Harden, J.W., Heimann, M., Howarth, R.W., Matson, P.A., McGuire, A.D., Melillo, J.M., Mooney, H.A., Neff, J.C., Houghton, R.A., Pace, M.L., Ryan, M.G., Running, S.W., Sala, O.E., Schlesinger, W.H., Schulze, E.D., 2006. Reconciling carbon-cycle concepts, terminology, and methods. Ecosystems 9, 1041–1050.
Charman, D.J., Beilman, D.W., Blaauw, M., Booth, R.K., Brewer, S., Chambers, F.M., Christen, J.A., Gallego-Sala, A., Harrison, S.P., Hughes, P.D.M., Jackson, S.T., Korhola, A., Mauquoy, D., Mitchell, F.J.G., Prentice, I.C., van der Linden, M., De Vleeschouwer, F., Yu, Z.C., Alm, J., Bauer, I.E., Corish, Y.M.C., Garneau, M., Hohl, V., Huang, Y., Karofeld, E., Le Roux, G., Loisel, J., Moschen, R., Nichols, J.E., Nieminen, T.M., MacDonald, G.M., Phadtare, N.R., Rausch, N., Sillasoo, U., Swindles, G.T., Tuittila, E.S., Ukonmaanaho, L., Väliranta, M., van Bellen, S., van Geel, B., Vitt, D.H., Zhao, Y., 2013. Climate-related changes in peatland carbon accumulation during the last millennium. Biogeosciences 10, 929–944.
Chaudhary, N., Westermann, S., Lamba, S., Shurpali, N., Sannel, A.B.K., Schurgers, G., Miller, P.A., Smith, B., 2020. Modelling past and future peatland carbon dynamics across the pan-Arctic. Global Change Biol. 26, 4119–4133.
Che, T., Li, X., Jin, R., Armstrong, R., Zhang, T., 2008. Snow depth derived from passive microwave remote-sensing data in China. Ann. Glaciol. 49, 145–154.
Chen, S., Liu, J., Wang, X., Zhao, S., Chen, J., Qiang, M., Liu, B., Xu, Q, Xia, D., Chen, F., 2021. Holocene dust storm variations over northern China: transition from a natural forcing to an anthropogenic forcing. Sci. Bull. 66, 2516–2527.
Clymo, R., 1984. The limits to peat bog growth. Philos. Trans. R. Soc. Lond. B Biol. Sci. 303, 605–654.
Davy, R., Esau, I., Chernokulsky, A.V., Outten, S., Zilitinkevich, S.S., 2017. Diurnal asymmetry to the observed global warming. Int. J. Climatol. 37, 79–93.
Friedlingstein, P., Cox, P., Betts, R., Bopp, L., Von Bloh, W., Brovkin, V., Cadule, P., Doney, S., Eby, M., Fung, I., Govindasamy, B., John, J., Jones, C., Joos, F., Kato, T., Kawamiya, M., Knorr, W., Lindsay, K., Matthews, H.D., Zeng, N., 2006. Climate–Carbon cycle feedback analysis: results from the C4MIP model intercomparison. J. Clim. 19, 3337–3353.
Frolking, S., Roulet, N.T., Moore, T.R., Richard, P.J.H., Lavoie, M., Muller, S.D., 2001. Modeling northern peatland decomposition and peat accumulation. Ecosystems 4, 479–498.
Frolking, S., Roulet, N.T., Tuittila, E., Bubier, J.L., Quillet, A., Talbot, J., Richard, P.J.H., 2010. A new model of Holocene peatland net primary production, decomposition, water balance, and peat accumulation. Earth Syst. Dynam. 1, 3–4.
Gallego-Sala, A.V., Charman, D.J., Brewer, S., Page, S.E., Prentice, I.C., Friedlingstein, P., Moreton, S., Amesbury, M.J., Beilman, D.W., Björck, S., Blyakharchuk, T., Bochicchio, C., Booth, R.K., Bunbury, J., Camill, P., Carless, D., Chimner, R.A., Clifford, M., Cressey, E., Courtney-Mustaphi, C., De Vleeschouwer, F., de Jong, R., Fialkiewicz-Koziel, B., Finkelstein, S.A., Garneau, M., Githumbi, E., Hribjlan, J., Holmquist, J., Hughes, P.D.M., Jones, C., Jones, M.C., Karofeld, E., Klein, E.S., Kokfelt, U., Korhola, A., Lacourse, T., Le Roux, G., Lamentowicz, M., Large, D., Lavoie, M., Loisel, J., Mackay, H., MacDonald, G.M., Makila, M., Magnan, G., Marchant, R., Marcisz, K., Martínez Cortizas, A., Massa, C., Mathijssen, P., Mauquoy, D., Mighall, T., Mitchell, F.J.G., Moss, P., Nichols, J., Oksanen, P.O., Orme, L., Packalen, M.S., Robinson, S., Roland, T.P., Sanderson, N.K., Sannel, A.B.K., Silva-Sánchez, N., Steinberg, N., Swindles, G.T., Turner, T.E., Uglow, J., Väliranta, M., van Bellen, S., van der Linden, M., van Geel, B., Wang, G., Yu, Z., Zaragoza-Castells, J., Zhao, Y., 2018. Latitudinal limits to the predicted increase of the peatland carbon sink with warming. Nat. Clim. Change 8, 907–913.
Gorham, E., 1991. Northern peatlands: role in the carbon cycle and probable responses to climatic warming. Ecol. Appl. 1, 182–195.
Hansen, J., Ruedy, R., Sato, M., Lo, K., 2010. Global surface temperature change. Rev. Geophys. 48, 1–29.
Hao, Z., Wu, M., Liu, Y., Zhang, X., Zheng, J., 2020. Multi-scale temperature variations and their regional differences in China during the Medieval Climate Anomaly. J. Geogr. Sci. 30, 119–130.
He, Y., Liu, W., Zhao, C., Wang, Z., Wang, H., Liu, Y., Qin, X., Hu, Q., An, Z., Liu, Z., 2013. Solar influenced late Holocene temperature changes on the northern Tibetan Plateau. Chin. Sci. Bull. 58, 1053–1059.
Hopple, A.M., Wilson, R.M., Kolton, M., Zalman, C.A., Chanton, J.P., Kostka, J., Hanson, P.J., Keller, J.K., Bridgham, S.D., 2020. Massive peatland carbon banks vulnerable to rising temperatures. Nat. Commun. 11, 2373.
Hou, J., D'Andrea, W.J., Liu, Z., 2012. The influence of ^{14}C reservoir age on interpretation of paleolimnological records from the Tibetan Plateau. Quat. Sci. Rev. 48, 67–79.
Ingram, H.A.P., 1982. Size and shape in raised mire ecosystems: a geophysical model. Nature 297, 300–303.
IPCC, 2021. In: Masson-Delmotte, V., Zhai, P., Pirani, A., Connors, S.L., Péan, C., Berger, S., Caud, N., Chen, Y., Goldfarb, L., Gomis, M.I., Huang, M., Leitzell, K., Lonnoy, E., Matthews, J.B.R., Maycock, T.K., Waterfield, T., Yelekçi, O., Yu, R., Zhou, B. (Eds.), Climate Change 2021: the Physical Science Basis. Contribution of Working Group I to the Sixth Assessment Report of the Intergovernmental Panel on Climate Change. Cambridge University Press.
IPCC, 2014. 2013 Supplement to the 2006 IPCC Guidelines for National Greenhouse Gas Inventories: Wetlands. IPCC, Switzerland.
Jones, M.C., Yu, Z., 2010. Rapid deglacial and early Holocene expansion of peatlands in Alaska. Proc. Natl. Acad. Sci. U.S.A. 107, 7347–7352.
Joosten, H., Sirin, A., Couwenberg, J., Laine, J., Smith, P., 2016. The role of peatlands in climate regulation. In: Bonn, A., Allott, T., Evans, M., Joosten, H., Stoneman, R. (Eds.), Peatland Restoration and Ecosystem Services: Science, Policy and Practice. Cambridge University Press, London, pp. 63–76.
Kuang, X., Jiao, J., 2016. Review on climate change on the Tibetan Plateau during the last half century. J. Geophys. Res. Atmos. 121, 3979–4007.
Kylander, M.E., Martínez-Cortizas, A., Bindler, R., Kaal, J., Sjöström, J.K., Hansson, S.V., Silva-Sánchez, N., Greenwood, S.L., Gallagher, K., Rydberg, J., Mörth, C.-M., Rauch, S., 2018. Mineral dust as a driver of carbon accumulation in northern latitudes. Sci. Rep. 8, 6876.
Leifeld, J., Menichetti, L., 2018. The underappreciated potential of peatlands in global climate change mitigation strategies. Nat. Commun. 9, 1071.
Liu, J., Wang, B., Cane, M.A., Yim, S.-Y., Lee, J.-Y., 2013. Divergent global precipitation changes induced by natural versus anthropogenic forcing. Nature 493, 656–659.
Loisel, J., Yu, Z., 2013a. Holocene peatland carbon dynamics in Patagonia. Quat. Sci. Rev. 69, 125–141.
Loisel, J., Yu, Z., 2013b. Recent acceleration of carbon accumulation in a boreal peatland, south central Alaska. J. Geophys. Res. Biogeo 118, 41–53.
Loisel, J., Yu, Z., Beilman, D.W., Camill, P., Alm, J., Amesbury, M.J., Anderson, D., Andersson, S., Bochicchio, C., Barber, K., 2014. A database and synthesis of northern peatland soil properties and Holocene carbon and nitrogen accumulation. Holocene 24, 1028–1042.
Moberg, A., Sonechkin, D.M., Holmgren, K., Datsenko, N.M., Karlen, W., Lauritzen, S.E., 2005. Highly variable Northern Hemisphere temperatures reconstructed from low- and high-resolution proxy data. Nature 433, 613–617.
Morris, P.J., Swindles, G.T., Valdes, P.J., Ivanovic, R.F., Gregoire, L.J., Smith, M.W., Tarasov, L., Haywood, A.M., Bacon, K.L., 2018. Global peatland initiation driven by regionally asynchronous warming. Proc. Natl. Acad. Sci. U.S.A. 115, 4851–4856.
Neukom, R., Steiger, N.J., Gomeznavarro, J.J., Wang, J., Werner, J.P., 2019. No evidence for globally coherent warm and cold periods over the preindustrial Common Era. Nature 571, 550–554.
Ramsey, C.B., 2008. Deposition models for chronological records. Quat. Sci. Rev. 27, 42–60.
Schurer, A.P., Mann, M.E., Hawkins, E., Tett, S.F.B., Hegerl, G.C., 2017. Importance of the pre-industrial baseline for likelihood of exceeding Paris goals. Nat. Clim. Change 7, 563–567.
Smith, L.C., Macdonald, G.M., Velichko, A.A., Beilman, D.W., Borisova, O.K., Frey, K.E., Kremenetski, K.V., Sheng, Y., 2004. Siberian peatlands a net carbon sink and global methane source since the early Holocene. Science 303, 353–356.
Spahni, R., Joos, F., Stocker, B.D., Steinacher, M., Yu, Z.C., 2013. Transient simulations of the carbon and nitrogen dynamics in northern peatlands: from the Last Glacial Maximum to the 21st century. Clim. Past 9, 1287–1308.
Treat, C.C., Kleinen, T., Broothaerts, N., Dalton, A.S., Dommain, R., Douglas, T.A., Drexler, J.Z., Finkelstein, S.A., Grosse, G., Hope, G., Hutchings, J., Jones, M.C., Kuhry, P., Lacourse, T., Lähteenoja, O., Loisel, J., Notebaert, B., Payne, R.J., Peteet, D.M., Sannel, A.B.K., Stelling, J.M., Strauss, J., Swindles, G.T., Talbot, J., Tarnocai, C., Verstraeten, G., Williams, C.J., Xia, Z., Yu, Z., Väliranta, M., Hättestrand, M., Alexanderson, H., Brovkin, V., 2019. Widespread global peatland establishment and persistence over the last 130,000 y. Proc. Natl. Acad. Sci. U.S.A. 116, 4822–4827.
Wang, J., Yang, B., Qin, C., Kang, S., He, M., Wang, Z., 2014a. Tree-ring inferred annual mean temperature variations on the southeastern Tibetan Plateau during the last millennium and their relationships with the Atlantic Multidecadal Oscillation. Clim. Dynam. 43, 627–640.
Wang, M., Chen, H., Wu, N., Peng, C., Zhu, Q., Zhu, D., Yang, G., Wu, J., He, Y., Gao, Y., 2014b. Carbon dynamics of peatlands in China during the Holocene. Quat. Sci. Rev. 99, 34–41.
Wilson, R.M., Hopple, A.M., Tfaily, M.M., Sebestyen, S.D., Schadt, C.W., Pfeifer-Meister, L., Medvedeff, C., McFarlane, K.J., Kostka, J.E., Kolton, M., Kolka, R.K., Kluber, L.A., Keller, J.K., Guilderson, T.P., Griffiths, N.A., Chanton, J.P., Bridgham, S.D., Hanson, P.J., 2016. Stability of peatland carbon to rising temperatures. Nat. Commun. 7, 13723.
Yang, B., Qin, C., Wang, J., He, M., Melvin, T.M., Osborn, T.J., Briffa, K.R., 2014. A 3,500-year tree-ring record of annual precipitation on the northeastern Tibetan Plateau. Proc. Natl. Acad. Sci. U.S.A. 111, 2903–2908.
Yao, T., Xue, Y., Chen, D., Chen, F., Thompson, L.G., Cui, P., Koike, T., Lau, W.K.M., Lettenmaier, D.P., Mosbrugger, V., 2019. Recent Third Pole's rapid warming accompanies cryospheric melt and water cycle intensification and interactions between monsoon and environment: multidisciplinary approach with observations, modeling, and analysis. Bull. Am. Meteorol. Soc. 100, 423–444.
Young, D.M., Baird, A.J., Gallego-Sala, A.V., Loisel, J., 2021. A cautionary tale about using the apparent carbon accumulation rate (aCAR) obtained from peat cores. Sci. Rep. 11, 9547.

Yu, Z., 2011. Holocene carbon flux histories of the world's peatlands: global carbon-cycle implications. Holocene 21, 761–774.
Yu, Z., 2012. Northern peatland carbon stocks and dynamics: a review. Biogeosciences 9, 4071–4085.
Yu, Z., Loisel, J., Brosseau, D.P., Beilman, D.W., Hunt, S.J., 2010. Global peatland dynamics since the last glacial maximum. Geophys. Res. Lett. 37, 1–5.
Yu, Z., Turetsky, M.R., Campbell, I.D., Vitt, D.H., 2001. Modelling long-term peatland dynamics. II. Processes and rates as inferred from litter and peat-core data. Ecol. Model. 145, 159–173.
Yu, Z., Vitt, D.H., Campbell, I.D., Apps, M.J., 2003. Understanding Holocene peat accumulation pattern of continental fens in western Canada. Can. J. Bot. 81, 267–282.
Zhang, H., Väliranta, M., Piilo, S., Amesbury, M.J., Aquino-López, M.A., Roland, T.P., Salminen-Paatero, S., Paatero, J., Lohila, A., Tuittila, E.S., 2020. Decreased carbon accumulation feedback driven by climate-induced drying of two southern boreal bogs over recent centuries. Global Change Biol. 26, 2435–2448.
Zhao, Y., Yu, Z., Tang, Y., Li, H., Yang, B., Li, F., Zhao, W., Sun, J., Chen, J., Li, Q., 2014. Peatland initiation and carbon accumulation in China over the last 50,000 years. Earth Sci. Rev. 128, 139–146.
Zhou, S., Wang, J., Xu, L., Wang, X., Colgan, P.M., Mickelson, D.M., 2010. Glacial advances in southeastern Tibet during late Quaternary and their implications for climatic changes. Quat. Int. 218, 58–66.